Biochimica et Biophysica Acta, 503 (1978) 304—315

BBA 47534

MECHANISM OF GENERATION AND REGULATION OF PHOTOPOTENTIAL BY BACTERIORHODOPSIN IN BIMOLECULAR LIPID MEMBRANE

THE QUENCHING EFFECT OF BLUE LIGHT

P. ORMOS, Zs. DANCSHÁZY and B. KARVALY

Institute of Biophysics, Biological Research Center, Hungarian Academy of Sciences, H-6701 Szeged, Odesszai krt. 62., P.O. Box 521 (Hungary)

(Received December 16th, 1977)

Summary

Photoelectric properties of bacteriorhodopsin incorporated into a bimolecular lipid membrane were investigated with special regard to the mechanism of photoelectric field generation. It was shown that besides its proton pump and electric generator functions bacteriorhodopsin works as a possible molecular regulator of the light-induced membrane potential. When a bimolecular lipid membrane containing bacteriorhodopsin is continuously illuminated in its main visible absorption band, and afterwards by superimposed blue light matching the absorption band of the long-living photobleached bacteriorhodopsin (M_{412}) as well, the latter either enhances or decreases the steady-state photoresponse, depending upon the intensity of the green light. Thus, the additional blue-light illumination tends to cause the resultant photoelectric membrane potential to become stabilized. Two alternative schemes are tentatively proposed for the photochemical cycle of bacteriorhodopsin whereby blue light can control photovoltage generation. A kinetic model of the proton pump and the regulation of the photoelectric membrane potential is presented. This model fits all the experimental findings, even quantitatively. From the model some kinetic and physical parameters of this light-driven pump could be determined.

Introduction

Since the discovery of bacteriorhodopsin [1] much detailed information has been obtained about its chemical and physical structures, functions, biochemical role, etc. The main function of bacteriorhodopsin is that it works

as a proton pump [2], transforming light energy into electrochemical energy stored in a proton gradient across the membrane. The generation of a light-induced proton gradient by bacteriorhodopsin has been demonstrated both in intact cells [2—5] and in model systems [6—10]. The simultaneous development of a light-induced membrane potential has also received experimental support [3—5,11—26]. On a bilayer lipid membrane containing purple patches in an oriented fashion (in the following: membranes with bacteriorhodopsin) [17,18] it has recently been shown that additional blue light above a green background illumination is capable of regulating the light-induced membrane potential [26].

The present paper deals with the details of the mechanism of this regulatory effect and its possible connections with the photochemical cycle of bacteriorhodopsin.

Materials and Methods

Purple membrane patches containing bacteriorhodopsin were prepared from the NRL R_1M_1 mutant strain of *Halobacterium halobium*, according to Oesterhelt and Stoeckenius [27]. Oriented incorporation of bacteriorhodopsin into a positively charged bilayer was achieved as described earlier [18]. Bimolecular lipid membranes were made from a decane solution of high-purity egg-yolk lecithin and octadecylamine (Merck, G.F.R.) (4% lecithin + 0.025% octadecylamine) over a hole of 1.5 mm diameter in the middle wall of a Teflon chamber, between two aqueous compartments with 10 mM NaCl solution. After thinning-down of the membrane, 10—30 μl of concentrated purple membrane suspension was introduced into one of the aqueous compartments, while the electrolyte solutions were vigorously stirred. Two identical calomel electrodes (OP 815, Radelkis, Hungary) were immersed in the bathing solutions and the electric circuit was completed through a Keithley Type 604 high-impedance electrometer connected to a Kipp and Zonen Type BD-5 fast micrograph. The electronic circuit allowed 0.01 mV sensitivity in voltage mode; the noise level was below 0.005 mV. The incorporation process was followed by the development of the photoresponse in time. It usually took place within 30—50 min, while the dark resistance of the membrane dropped to about half that of the unmodified membrane (10^8 Ω cm^2). These membranes possessed a fairly long life-time, usually several hours, and in further studies only those membranes were used of which the dark and photoelectric characteristic did not change appreciably with time after the incorporation had ended. Dark resistance and photoresponse under arbitrarily chosen "standard" conditions were used to judge the states of membranes with bacteriorhodopsin during long-run measurements. The membranes were excited through a double-beam optical set-up as described previously [26]. With the use of efficient heat-filters in both light pathways, the changes in temperature near the membrane were less than 0.5° C, even at the highest light intensities used. "Monochromatic" light beams were usually selected from the light of 200 W high-pressure mercury vapor lamps (HBO 200, Narva, G.D.R.), using BG 12 and VG4 broad-band glass filters (Zeiss, Jena, G.D.R.) [26]. The average number of incident photons were calculated for the main mercury lines transmitted by the filters in the corres-

ponding band, taking into account the relative intensities of lines. The photovoltaic action spectra of these membranes followed the absorption spectrum of bacteriorhodopsin quite satisfactorily in the visible region [18]. The reproducibility of the photoelectric measurements on a given membrane was usually better than 5% above 2 mV, and 10% for lower signal levels. The compartment without purple membrane was always positive when illuminated. Membranes without bacteriorhodopsin exhibited no photoelectric response. All membranes with bacteriorhodopsin displayed the same photoelectric properties; only the amplitude of the photoresponse varied by about 30—50% from system to system. Due to the frequent and prolonged illumination of bacteriorhodopsin incorporated into the membrane, all the experiments here obviously concern the light-adapted form of bacteriorhodopsin (BR_{570}). In general, the notations of Lozier et al. [7,28] will be used for the different bacteriorhodopsin species occurring in the fundamental photochemical cycle; Litvin and Balashov's [29] assignments (P species) will be applied, however, to the blue-light-generated photoproducts of M_{412}. All the measurements were carried out at constant temperature (22 ± 1°C) in a darkened room. Light intensities at the membrane were measured with a calibrated Tektronix Type J16 digital photometer.

Results

The time courses of the photoelectric response were qualitatively similar for excitations with different wavelengths. The sign of the photovoltage was the same and its intensity dependence (more correctly quantum flow density dependence) was of sigmoid type and very similar for all monochromatic excitations. (In these experiments metal interference filters with 10 nm bandwidth were applied.) The development of the photovoltaic response (at the available time resolution) displayed monophasic, saturation-like kinetics with excitation-dependent rise-time and saturation level (U_{photo}). For white-light illumination the slope of the dependence of U_{photo} upon light intensity was found less than that for monochromatic excitation.

When a second blue-light excitation was superimposed on the green one, an additional photoeffect could be detected (Fig. 1). With increasing green-light intensity the resultant U_{photo} was at first larger than that for green-light excitation alone, then at a certain green-light illumination level it remained unchanged, and afterwards it became smaller (Fig. 1). The variation of the quenching of the green-light-induced photoresponse with the intensity of the blue light is plotted in Fig. 2 at a constant green-light level, obtained in a separate set of measurements. The quenching by blue light exhibited a maximum when the intensity of the green light was varied; this shifted towards higher green-light intensities when the number of incident blue photons increased. The dependence of the resultant U_{photo} upon the intensity of the green light is given in Fig. 3. The blue-light-induced photoeffect changed its sign at a characteristic quantum flow density of the incident green light (the intercept) for all membranes, irrespective of the intensity of the blue light.

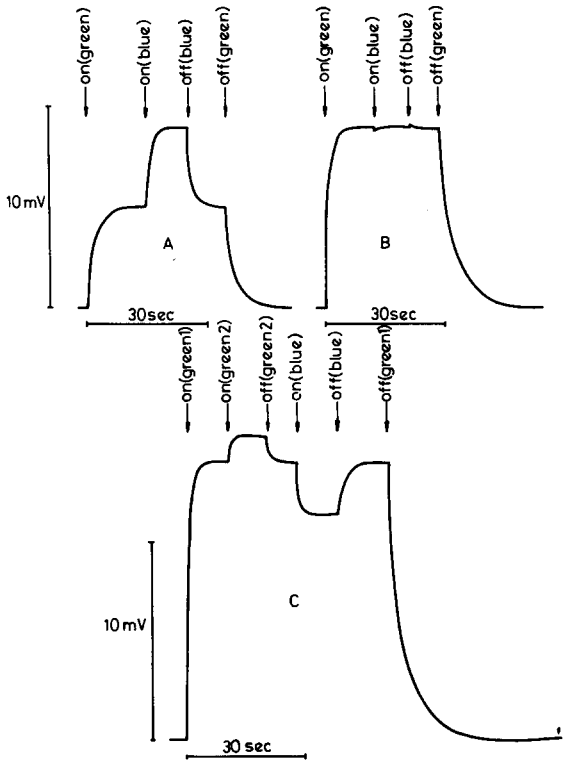

Fig. 1. Time-course of the photopotential of a bimolecular lipid membrane with bacteriorhodopsin upon simultaneous excitation by green and blue lights at different green-light intensities. The light intensities were:

(A) $I_g = 2.2 \cdot 10^{20}$ photons $\cdot$ m$^{-2} \cdot$ s^{-1}, $I_b = 10^{22}$ photons $\cdot$ m$^{-2} \cdot$ s^{-1}

(B) $I_g = 7.9 \cdot 10^{20}$ photons $\cdot$ m$^{-2} \cdot$ s^{-1}; $I_b = 10^{22}$ photons $\cdot$ m$^{-2} \cdot$ s^{-1}

(C) $I_g(1) = 5.8 \cdot 10^{21}$ photons $\cdot$ m$^{-2} \cdot$ s^{-1}; $I_g(2) = 3 \cdot 10^{21}$ photons $\cdot$ m$^{-2} \cdot$ s^{-1}, $I_b = 10^{22}$ photons $\cdot$ m$^{-2} \cdot$ s^{-1}.

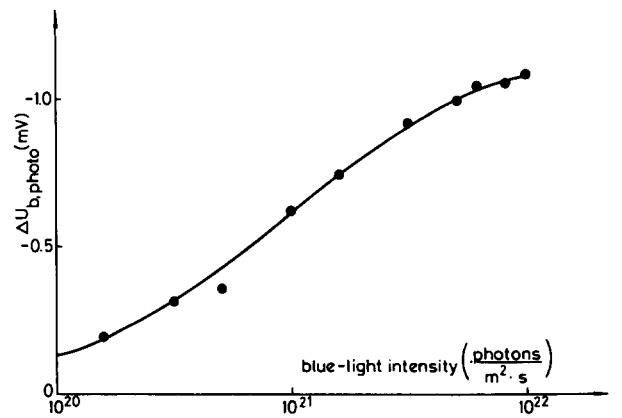

Fig. 2. Dependence of the blue-light-induced quenching of the green-light-induced photopotential ($\Delta U_{b,photo}$) upon the blue-light intensity at constant green background illumination. $I_g = 3 \cdot 10^{21}$ photons $\cdot$ m$^{-2} \cdot$ s^{-1}.

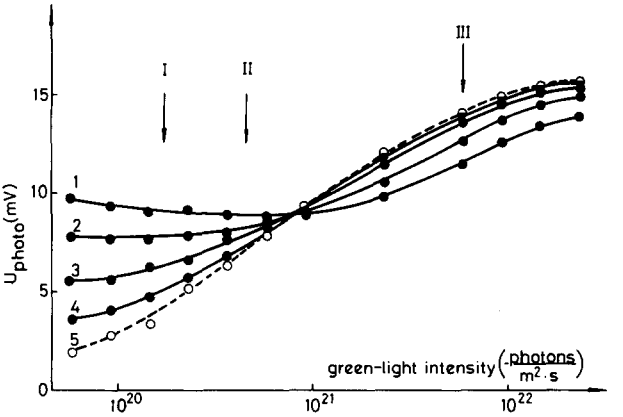

Fig. 3. Dependence of the resultant photopotential (U_{photo}) induced by simultaneous green- and blue-light illumination upon the green-light intensity at different constant blue-light intensities. The blue light intensities were:

1, $I_b = 10^{22}$ photons $\cdot$ m$^{-2} \cdot$ s^{-1};

2, $I_b = 2.7 \cdot 10^{21}$ photons $\cdot$ m$^{-2} \cdot$ s^{-1}; 3, $I_b = 7.2 \cdot 10^{20}$ photons $\cdot$ m$^{-2} \cdot$ s^{-1};

4, $I_b = 1.9 \cdot 10^{20}$ photons $\cdot$ m$^{-2} \cdot$ s^{-1}; 5, $I_b = 0$.

The arrows I, II and III indicate the sun light intensities in the green spectral region used in our experiments, measured in the early morning, at noon in scattered light and at noon in bright sunshine, respectively, in Szeged in March.

Discussion

Although the photochemical cycle of bacteriorhodopsin has been fairly well established, little is known about the connection of photochemistry and membrane processes such as proton translocation, the nature of the photoelectric potential, etc. The recognition of the above regulatory effect [26] offered a good possibility for correlating photochemical and membrane processes, using the reconstitution technique [18].

Since the intensity dependence of U_{photo} obtained with white-light illumination has a slope less than that for monochromatic green-light excitation, at least one spectral component of the white light should have an unusual non-additive effect on the resultant photoresponse. The excitation of the blue-absorbing product, M_{412}, by light is known to affect the kinetics of the photochemical cycle [30—34]. Therefore, it was reasonable to search for the particular effects of secondary excitations with blue light on the green-light-induced (primary) photopotential. Figs. 1 and 3 provide clear-cut evidence that above a certain level of green-light intensity the additionally applied blue light is capable of reducing the primary photovoltage. As seen in Fig. 1c, considerable quenching of the primary U_{photo} occurs ever when the intensity of the green light is much lower than the saturation value. Evidently, the drop in the resultant U_{photo} due to the additional blue light cannot be attributed to an "oversaturation effect" as found for high intensity white-light excitation of the proteoliposome-planar lipid membrane containing bacteriorhodopsin [14].

It has been shown that the photochemical cycle can be accelerated by appropriate blue light [29,33,34]. Hence, one might conclude that the proton pump

can also be accelerated by blue light. However, the observed quenching effect makes improbable the possibility of increasing the velocity of the proton pump. It is therefore to be assumed that, although the photochemical turnover can be speeded up, most of the blue-light-accelerated cycles are inefficient from the point of view of pumping protons. Consequently, in the photovoltage generation (which is inherently connected to proton translocation) blue light, depending upon the intensity of the green light, may have not an enhancing but a quenching effect.

It was previously proposed [26] that this phenomenon may offer a regulatory mechanism for the light-induced membrane potential. The simplified explanation of the regulation of U_{photo} by blue light was that the quenching must be connected with the presence of M_{412}, which may consist of several components with different life-times and absorption maxima around 410 nm [29,34]. In the following we shall consider M_{412} as a member(s) of this pool, involved in the acceleration of the photochemical cycle and in this particular photoelectric effect of blue light. The operation of the proton pump is based upon the overall photochemical reaction of bacteriorhodopsin:

$$h\nu + BR_{570} \rightarrow M_{412} + H^+ \qquad (I)$$

and the overall dark, temperature-limited recombination process:

$$M_{412} + H^+ \rightarrow BR_{570} \qquad (II)$$

Here $h\nu$ may denote any light quantum absorbed by BR_{570} with the corresponding cross-section. These two processes form the basis of the photoelectric responsiveness of bacteriorhodopsin. If the exciting light also contains a blue component, besides processes I and II the photochemical reaction

$$M_{412} + h\nu_b \rightarrow P_X \xrightarrow{H^+} BR_{570} \qquad (III)$$

also occurs, where $h\nu_b$ is a blue photon captured by M_{412} and P_X is an excitation product of M_{412} (possibly P_{421} [29]). This blue-light-facilitated reformation of BR_{570} leads to the decrease of the resultant U_{photo}, as demonstrated in Fig. 1c. Process III becomes predominant only above a certain intensity of the green light (determined by the corresponding absorption cross-sections of BR_{570} and M_{412}), irrespective of the intensity of the blue light (Figs. 2 and 3).

Two possible pathways have been proposed to explain why the photochemical cycles are ineffective [26]: (1) In the course of the reformation of BR_{570}, protons are picked up by species P_X from that side of the membrane to which they are injected, and thus P_X works as an H^+-trap. (2) P_X inhibits proton release and functions as a shunt of the proton pump.

In order for the experimental results to be interpreted, a certain completion of the photochemical cycle becomes necessary. Almost nothing is known about the location of proton-releasing and/or capturing "active sites" of different photochemical intermediates in the membrane, so their positions towards the "inner" or "outer" side of the membrane in the schemes are merely postulated (Fig. 4). It is not clear either at which stage of the photochemical cycle the proton release takes place: whether before or simultaneously with the formation of M_{412}, or after it through a conformational intermediate. These

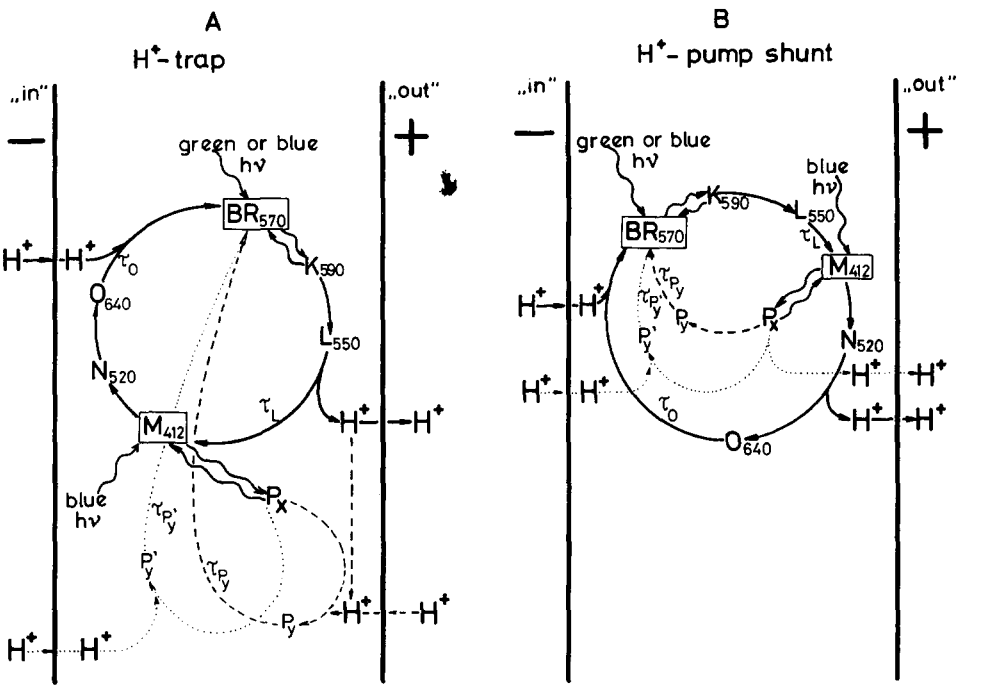

Fig. 4. Schemes representing the two possible mechanisms of the photopotential-quenching effect. The basic photochemical cycle of bacteriorhodopsin (solid line) is summarized according to literature data. The definition of the intermediates according to the literature is the following: BR_{570}, bacteriorhodopsin in dark, in the ground state; K_{590}, the first intermediate of the electronically excited BR_{570}; L_{550}, a dark intermediate before the formation of M_{412}; M_{412}, the first long living intermediate with deprotonated Schiff-base; N_{520}, dark intermediate; O_{640}, the last intermediate before the reformation of BR_{570}. In the regulatory cycles (dashed and dotted lines) the definitions of the intermediates are the followings: P_X, the first intermediate of the electronically excited M_{412}; P_Y and P'_Y, dark intermediates before the formation of BR_{570}. The respective life-times of the rate-limiting intermediates are indicated by τ in the figure. For further explanation see text.

two possible routes are the bases of the H^+-trap (Fig. 4A) and the H^+-shunt (Fig. 4B) mechanisms, respectively.

H^+-trap

When the photochemical cycle runs on the basic pathway (Fig. 4A, solid line), after electronic excitation, BR_{570} turns first into its bathoform (K_{590}) in a photoreversible step, which finally forms M_{412}. During this semi-cycle a proton is removed from the Schiff-base and then either released into the aqueous phase or retained in the lipoprotein matrix. In the following, a distinction will not be made between these two theoretical possibilities, the model to be proposed not being sensitive to them.

Under usual conditions a dark product of M_{412} picks up one proton from the "inner side" and regenerates BR_{570}. As a result of the basic photochemical cycle, therefore, one proton is pumped through the membrane from "inside" to "outside". Upon absorption of a blue quantum by M_{412}, the first intermediate after excitation, P_X (possibly P_{421}), is formed in a photoreversible step, and is reconverted into BR_{570} through intermediates either P_Y or P'_Y (possibly

P_{585}) [29,34], with respective probabilities η and $1-\eta$, while one proton is taken up from either the "outer" or the "inner" side of the membrane, respectively (dashed and dotted lines in Fig. 4A). Those cycles which run via the pathway $M_{412} \rightarrow P_X \rightarrow P_Y \rightarrow BR_{570}$, i.e. when P_Y picks up a proton from the "outer side", do not contribute to the proton gradient.

H^+-pump shunt

In the basic cycle (solid line in Fig. 4B) of this scheme the proton release occurs between the intermediates N_{520} and O_{640} following the formation of M_{412}. BR_{570} is regenerated by taking up one proton from the "inner side". If P_X is formed upon blue-light excitation, it is reconverted through P_Y to BR_{570} without proton release, with probability η (dashed line). However, it cannot be excluded that P_X returns to the purple form through P'_Y, with probability $1-\eta$, releasing one proton into the "outer side" and thus contributing to the pH gradient (dotted line).

Consequently, η is the efficiency of the quenching in both schemes, or, in turn, $1-\eta$ means the efficiency of the acceleration of the proton pump by blue light.

Kinetic model

Now, the photochemical cycle and proton translocation being connected, a kinetic model will be given below for the generation and regulation of a light-induced membrane potential. It is assumed that bacteriorhodopsin molecules participate in proton translocation independently and that the photochemical cycle consists of elementary reactions, considered as irreversible and of first-order kinetics. As regards the kinetics of the photochemical cycle and the proton-pump model, both quenching schemes (H^+-trap, H^+-shunt) lead to the same results. So through the quantitative analysis no distinction will be made between them. For the sake of simplicity only the dominant intermediates, i.e. those possessing the longest life-times, will be taken into account in the respective branches of the cycles. The kinetics of the photochemical cycle can then be described by the following set of differential equations:

$$\frac{d[BR_{570}]}{dt} = -(I_g\sigma_g + I_b\sigma_b)[BR_{570}] + \frac{1}{\tau_{P_y}}[P_y] + \frac{1}{\tau_{P'_y}}[P'_y] + \frac{1}{\tau_0}[M_{412}] \tag{1}$$

$$\frac{d[L_{550}]}{dt} = (I_g\sigma_g + I_b\sigma_b)[BR_{570}] - \frac{1}{\tau_L}[L_{550}] \tag{2}$$

$$\frac{d[M_{412}]}{dt} = \frac{1}{\tau_L}[L_{550}] - I_b\sigma_b^*[M_{412}] - \frac{1}{\tau_0}[M_{412}] \tag{3}$$

$$\frac{d[P_y]}{dt} = \eta I_b\sigma_b^*[M_{412}] - \frac{1}{\tau_{P_y}}[P_y] \tag{4}$$

$$\frac{d[P'_y]}{dt} = (1-\eta)I_b\sigma_b^*[M_{412}] - \frac{1}{\tau_{P'_y}}[P'_y] \tag{5}$$

and

$$[BR_{570}]_0 = [BR_{570}] + [L_{550}] + [M_{412}] + [P_y] + [P'_y] \tag{6}$$

where I_g and I_b are the intensities of green and blue light, respectively; σ_g, σ_b and σ_b^* are the absorption cross-sections multiplied by the photochemical quantum efficiencies of BR_{570} for the green and the blue lights, and that of M_{412} for blue light, respectively; $[BR_{570}]_0$ is the average surface concentration of BR_{570} on the membrane able to participate in proton translocation; and $[BR_{570}]$, $[L_{550}]$, $[M_{412}]$, $[P_Y]$ and $[P'_Y]$ are surface concentrations and τ_{570}, τ_{412}, τ_{P_Y} and $\tau_{P'_Y}$ are the life-times of the intermediates in Fig. 4. In these kinetic equations it was presumed that $\tau_{P_Y} = \tau_{P'_Y}$. Upon solution of this set of equations, the steady-state concentration of M_{412} can be expressed as

$$[M_{412}] = [BR_{570}]_0 \frac{I_g\sigma_g + I_b\sigma_b}{1 + \tau_L(I_g\sigma_g + I_b\sigma_b)} \cdot \frac{1}{\frac{I_g\sigma_g + I_b\sigma_b}{1 + \tau_L(I_g\sigma_g + I_b\sigma_b)}(1 + \tau_{P_y} I_b\sigma_b^*) + \frac{1}{\tau_0} + I_b\sigma_b^*} \tag{7}$$

To define the number of protons pumped through the membrane in unit time, one has to calculate the number of photochemical cycles per second (f) completed in the efficient pathways:

$$f = \frac{1}{\tau_0}[M_{412}] + (1 - \eta)I_b\sigma_b^*[M_{412}] \tag{8}$$

where η is the efficiency as introduced above. As a result of the vectorial proton translocation, a proton concentration difference $2\Delta c$ is built up between the opposite interfaces of the membrane, which drives a passive back-diffusion (leakage) of protons as well. This latter is assumed to be proportional to $2\Delta c$, with a factor α characteristic of the membrane (proton permeability, etc.). When the steady state is reached, the active (pumped) and the passive (leaked) proton flows are equal, and then

$$\frac{1}{\tau_0}[M_{412}] + (1 - \eta)I_b\sigma_b^*[M_{412}] = 2\alpha\Delta c \tag{9}$$

i.e. Δc is proportional to the net electric charge appearing in the interfacial region, with different signs on opposite sides. Δc charges up the capacitance of the membrane considered as a plate condenser and so the U_{photo} appearing is

$$P_{photo} = \frac{\beta}{2\alpha}\left(\frac{1}{\tau_0} + (1 - \eta)I_b\sigma_b^*\right)[M_{412}] \tag{10}$$

where β is practically the inverse capacity of the membrane.

Comparison of theory and experiment

As seen from Eqns. 7 and 10, $[BR_{570}]_0\ \beta/2\alpha$ is only an amplitude factor that has no further effect on the characteristics of the curves, which are determined entirely by the molecular parameters σ, τ and η. Therefore, one does not have to pay attention to the amplitude factor in the course of fitting. In the numerical calculations the procedure below was followed:

On the basis of the only coherent pair of data for τ_L and τ_0, the values $\tau_L = 30\ \mu s$ and $\tau_0 = 10$ ms were tentatively accepted. σ_g (the product of the

absorption cross-section and the photochemical quatum efficiency) was chosen as $3 \cdot 10^{-17}$ cm^2 [35]. These values were kept constant throughout the calculations. σ_b and σ_b^* caould be varied only in a narrow range, since they are strongly connected with the corresponding absorption cross-sections. The room temperature value of τ_{P_Y} is not known, measurements having been made either in ether solutions or at low temperature [29—31]. Thus, the only parameters which could be freely varied were τ_{P_Y} and η. In the case of the best fit the following parameter values were obtained:

$\sigma_b = 1.5\ 10^{-17}$ cm^2 ± 20%; $\sigma_b^* = 0.9 \cdot 10^{-17}$ cm^2 ± 20%

$\tau_{P_y} = 75\ \mu$s ± 30%; $\eta = 1 - 5\%$

Since (1) the σ parameters include the corresponding photochemical quantum efficiencies, which are mostly unknown and certainly different for different intermediates, and (2) the excitations were not in fact rigorously monochromatic (see Materials and Methods) as assumed in the calculations, the above values for σ_b and σ_b^* seem quite reasonable [36]. The τ_{P_Y} obtained indicates that the blue-light-induced, $M_{412} \rightarrow P_X \rightarrow BR_{570}$ pathway has a temperature-limited step with a time constant of the order of μs. As the most convincing fit was obtained at $\eta = 1$, i.e. when pratically all cycles which are completed by exciting M_{412} with blue light are lost for pumping protons, the H^+-pump shunt model (Fig. 4B) appears more plausible. For comparison of the theory and experiments, the simulated curves obtained with optimum fitting and the experimental results are plotted in Fig. 5, which is an equivelent representation of Fig. 3. It is obvious that the theory describes the experimental observations even quantitatively over the wole intensity regions of the green and blue lights used, and the calculated curves have all the basic features of the measured

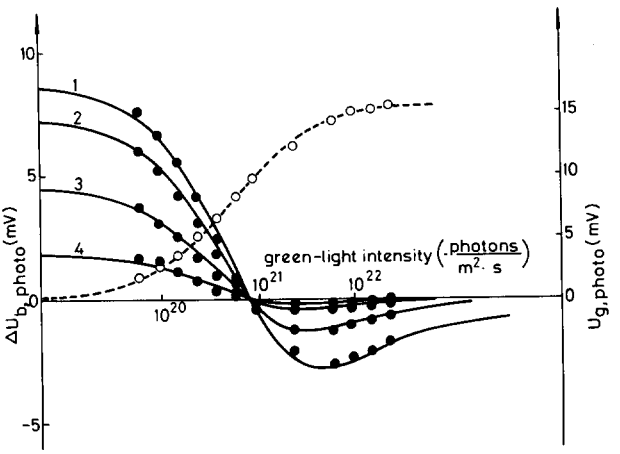

Fig. 5. Fitting of the measured data to the calculated model. Dependence of the green-light-induced photopotential ($U_{g'photo}$) on the intensity of the incident green light (○, measured; - - - - -, calculated), and the dependence of the blue-light-induced additional photopotential ($\Delta U_{b'photo}$) on the green-light intensity (●, measured; ———, calculated) at different constant blue-light intensities. For blue-light intensities see Fig. 3. Detailed explanation is given in the text.

ones (intercept, shift of the minimum towards higher green-light excitation levels on increase of the blue-light intensity, etc.). It is easy to see that, in agreement with Figs. 3 and 5, the characteristic quantum flow density (I'_g) of the green light, above which concomitant blue-light illumination starts decreasing the resultant U_{photo}, irrespective of its intenstity, is determined by intrinsic photochemical parameters of the bacteriorhodopsin molecule, and

$$I'_g = \frac{1}{\tau_0 \alpha_g} \cdot \frac{\sigma_b}{\sigma_b^*} \tag{11}$$

On insertion of the corresponding numerical values used and/or obtained in the above calculations, Eqn. 11 yields $I'_g = 5 \cdot 10^{22}$ photons $\cdot$ m^{-2} $\cdot$ s^{-1}, while from Figs. 3 and 5 it follows that $I'_g = 10^{21}$ photons $\cdot$ m^{-2} $\cdot$ s^{-1}. The apparently large difference is explained by the inevitable scattered light originating from the edge of the white Teflon support, which passes the membrane parallel to, rather than perpendicular to its surface. (The effect of the scattered light is comparable to the primary photoresponse due to the perpendicular incident light.) Accordingly, the agreement can be regarded as acceptable, and hence the proposed model faithfully interconnects the photochemical cycle and the charge separation as the basis of potential generation, while the observed photopotential is primarily due to the polarization of the double layer adjacent to the membrane.

Finally, the possible occurrence and role of the above-discussed phenomenon should be dealt with in its relation to the regulation of the light-induced membrane potential. As seen from Figs. 3 and 5, in the event of the simultaneous presence of blue and green components in the exciting beam the light-induced membrane potential is about 20% less sensitive to the changes in light intensity. This means that the mutual incidence of blue and green lights results in a certain stabilization and control of the membrane potential; the relevance of this in vital processes of halobacteria is not yet clear.

Acknowledgements

The authors wish to thank Professor V.P. Skulachev, Professor F.F. Litvin, Dr. Cs. Fajszi and Mr. Cs. Bagyinka for valuable critical remarks and discussions on the manuscript and to Mrs. E. Nagy for technical assistance.

References

1 Oesterhelt, D. and Stoeckenius, W. (1971) Nature New Biol. 233, 149–152
2 Oesterhelt, D. and Stoeckenius, W. (1973) Proc. Natl. Acad. Sci. U.S. 70, 2853–2857
3 Beljakova, T.N., Kadziauskas, J.P., Skulachev, V.P., Smirnova, I.A., Chekulaeva, L.N. and Jasaitis, A.A. (1975) Dokl. Akad. Nauk S.S.S.R. 223, 483–486
4 Bakker, E.P., Rottenberg, H. and Caplan, S.R. (1976) Biochim. Biophys. Acta 440, 557–572
5 Michel, H. and Oesterhelt, D. (1976) FEBS Lett. 65, 175–178
6 Racker, E. and Stoeckenius, W. (1974) J. Biol. Chem. 249, 662–663
7 Lozier, R.H., Niederberger, W., Bogomolni, R.A., Hwang, S.B. and Stoeckenius, W. (1976) Biochim. Biophys. Acta 440, 545–556
8 Eisenbach, M., Bakker, E.P., Korenstein, R. and Caplan, S.R. (1976) FEBS Lett. 71, 228–232
9 Renthal, R. and Lanyi, J.K. (1976) Biochemistry 10, 2136–2143

10 Happe, M., Teather, R.M., Overath, P., Knobling, A. and Oesterhelt, D. (1977) Biochim. Biophys. Acta 465, 415—420
11 Kayushin, L.P. and Skulachev, V.P. (1974) FEBS Lett. 39, 39—42
12 Drachev, L.A., Kaulen, A.D., Ostroumov, S.S. and Skulachev, V.P. (1974) FEBS Lett. 74, 43—45
13 Drachev, L.A., Jasaitis, A.A., Kaulen, A.D., Kondrashin, A.A., Liberman, E.A., Nemecek, I.B., Ostroumov, S.A., Semenov, A.Yu. and Skulachev, V.P. (1974) Nature 249, 321—324
14 Drachev, L.A., Frolov, V.N., Kaulen, A.D., Liberman, E.A., Ostroumov, S.A., Plakunova, V.G., Semenov, A.Yu. and Skulachev, V.P. (1976) J. Biol. Chem. 251, 7059—7065
15 Renthal, R. and Lanyi, J.K. (1975) Biophys. J. 15, 68a
16 Skulachev, V.P. (1976) FEBS Lett. 64, 23—25
17 Dancsházy, Zs. and Karvaly, B. (1976) International Conference of Photochemistry on Storage and Conversion of Solar Energy, Abstracts, p. F5, London, Ontario
18 Dancsházy, Zs. and Karvaly, B. (1976) FEBS Lett. 72, 136—138
19 Shieh, P. and Packer, L. (1976) Biochem. Biophys. Res. Commun. 71, 603—609
20 Herrmann, T.R. and Rayfield, G.W. (1976) Biochim. Biophys. Acta 443, 623—628
21 Blok, M.C., Hellingwerf, K.J. and Van Dam, K. (1977) FEBS Lett. 76, 45—50
22 Trissl, H.W. and Montal, M. (1977) Nature 266, 655—657
23 Stoeckenius, W., Hwang, S.B. and Korenbrot, J. (1976) Nobel Symposium. The Structure of Biological Membranes Skövde, June 7—11
24 Bamberg, E. (1977) Biophys. Struct. Mech. 3, 39—42
25 Korenbrot, J.I. (1977) Ann. Rev. Physiol. 39, 19—49
26 Karvaly, B. and Dancsházy, Zs. (1977) FEBS Lett. 76, 36—40
27 Oesterhelt, D. and Stoeckenius, W. (1974) Methods Enzymol. 31, 667—678
28 Lozier, R.H., Bogomolni, R.A. and Stoeckenius, W. (1975) Biophys. J. 15, 955—962
29 Litvin, F.F. and Balashov, S.P. (1977) Biofizika (in Russian) 22, 1111—1114
30 Oesterhelt, D. and Hess, B. (1973) Eur. J. Biochem. 37, 316—326
31 Hess, B. (1976) FEBS Lett. 64, 26—28
32 Oesterhelt, D., Gottschlich, R., Hartmann, R., Michel, H. and Wagner, G. (1977) Symposia of the Society for General Microbiology Number XXVII. Microbial Energetics, 1977, pp. 333—349
33 Hess, B., Kuschmitz, D. and Oesterhelt, D. (1976) IUB 10th International Congress of Biochemistry, Hamburg, Abstract 06-2-205, 06-2-206
34 Hess, B. and Kuschmitz, D. (1977) FEBS Lett. 74, 20—24
35 Goldschmidt, C.R., Ottolenghi, M. and Korenstein, R. (1976) Biophys. J. 16, 839—843
36 Becher, B. and Ebrey, T.G. (1977) Biophys. J. 17, 185—191